Extreme Rainstorm-Induced Cascading Vulnerability in Cross-Border Metro Networks: A Modeling Framework for Shenzhen-Hong Kong

Yangyang Meng
The Hong Kong Polytechnic University
yangyang.meng@polyu.edu.hk

Xiaofei Zhao
City University of Hong Kong
xf.zhao@my.cityu.edu.hk

ABSTRACT

Extreme rainstorms increasingly threaten cross-border metro systems whose interdependencies may amplify localized disruptions into systemic failures. This study proposes a network-based cascading vulnerability assessment framework for cross-border metro networks, motivated by the Shenzhen-Hong Kong system. The model integrates rainstorm-induced initial failures, probabilistic structural interdependency, dynamic load redistribution, and overload-driven cascading dynamics. A multidimensional vulnerability metric system quantifies structural, functional, and cascading impacts, together with a coupling-induced amplification factor. Conceptual validation on a dual-layer simplified network shows that cross-border coupling significantly amplifies system-wide degradation and exhibits threshold-like redundancy behavior. Compared with existing studies, this study identifies cross-border connectors as systemic vulnerability amplifiers and underscores the need for coordinated redundancy planning. Future work will extend the model to empirically grounded network data and spatially explicit rainfall scenarios. This study contributes to interdependent infrastructure risk modeling and provides a decision-support foundation for coordinated cross-border crisis management and resilience planning under extreme climate events.

Keywords

Metro network vulnerability; Cross-border interdependent networks; Extreme rainstorm disaster; Cascading failure dynamics; Crisis management and resilience.

INTRODUCTION

In the context of global climate change, extreme rainstorm events are exhibiting increasing intensity, higher frequency, and greater spatial uncertainty (Yang et al., 2025; D.-M. Zhang et al., 2025), particularly in coastal regions. Shenzhen and Hong Kong, as highly urbanized coastal cities, rely heavily on underground rail transit systems characterized by deep alignments and limited drainage capacity, rendering them especially vulnerable to short-duration, high-intensity rainfall (Liang et al., 2026; Liang & Guan, 2025). Recently, multiple extreme rainstorm events have significantly disrupted transportation networks in both cities. For example, in September 2023, Shenzhen experienced a historically unprecedented rainstorm that led to severe urban flooding, forcing several metro lines to suspend or restrict operations. Meanwhile, Hong Kong issued the black rainstorm warning signal, and several underground stations were temporarily closed due to inundation (Liang et al., 2026; Liang & Guan, 2025). The event completely paralyzed cross-border transportation between Shenzhen and Hong Kong and resulted in substantial economic losses. More importantly, it exposes the systemic vulnerability of cross-border rail systems under extreme rainfall conditions: beyond isolated infrastructure damage, cascading failures can propagate across interconnected networks, potentially triggering the breakdown of the entire cross-border coupled system (Chen et al., 2024; Wang et al., 2025).

The metro systems of Shenzhen and Hong Kong are physically interconnected through multiple border stations and cross-border rail links, forming a complex infrastructure network that spans administrative jurisdictions. This network exhibits the distinctive feature of high physical coupling with institutionally segmented governance.

While such a structure enhances connectivity and mobility integration, it also increases systemic interdependence. As a result, extreme rainstorm hazards may trigger cross-boundary cascading effects within the coupled network, undermining overall system resilience and constraining coordinated emergency response capacity (Borghetti & Marchionni, 2023). Accordingly, there is a pressing need to develop a vulnerability assessment framework for cross-border metro systems under extreme rainstorm scenarios, drawing on an integrated perspective that bridges complex systems theory and crisis management.

In recent years, the study of vulnerability and resilience in urban rail transit systems under disaster scenarios has become an important topic in the fields of complex networks and infrastructure risk analysis (Huang & Loo, 2023; Jiao et al., 2023; Jing et al., 2025; Liang et al., 2026; Rinaldi et al., 2001). Early research (Hong et al., 2022; Meng, 2024; Qi et al., 2022; J. Zhang et al., 2018) was largely grounded in complex network robustness theory, simulating node failures through random or targeted attacks and evaluating system degradation using structural indicators such as the proportion of the largest connected component and network efficiency. While these studies laid the foundation for understanding the topological characteristics of metro networks, they often overlooked the actual triggering mechanisms of real-world disasters. Subsequent research (Gao et al., 2024; Ma et al., 2023; Y. Zhang et al., 2020) incorporated passenger flow data and functional performance metrics, shifting attention toward service continuity and employing load-capacity models to characterize cascading failures (Wang et al., 2025). More recently, in the context of extreme climate events, some studies (Ansari et al., 2024; Li et al., 2025; Tian et al., 2024) have introduced hazard models (e.g., floods and earthquakes) into rail transit risk analysis to construct disaster-driven failure scenarios. However, existing research remains predominantly focused on single-city or single-layer network structures, with limited attention to the vulnerability of cross-border coupled systems.

At the same time, much of the complex network literature (Meng, 2024; Qi et al., 2022) lacks explicit modeling of exogenous shocks based on specific hazard scenarios, making it difficult to capture the spatial heterogeneity and physical triggering mechanisms of natural disasters such as extreme rainstorms. Although multidimensional resilience metrics, encompassing structural robustness, functional performance, and recovery capacity, have gradually evolved, a comprehensive evaluation framework tailored to cross-border coupled systems is still lacking. In particular, under cross-border infrastructure contexts characterized by physical interdependence but institutional separation, quantitative research on how disaster impacts are amplified into systemic risks through interdependent mechanisms remains limited. Therefore, it is necessary to develop an integrated analytical framework for cross-border metro systems that combine hazard-trigger modeling, interdependent cascading propagation mechanisms, and multidimensional vulnerability assessment, thereby addressing current gaps in cross-border risk transmission analysis and coordinated emergency response support.

Focusing on the risk propagation and system degradation processes of the Shenzhen-Hong Kong (SZ-HK) cross-border metro system under extreme rainstorms, this paper proposes a modeling framework oriented toward crisis management of cross-border infrastructure systems. The main contributions are as follows:

- A dual-layer cross-border coupled metro network model of the SZ-HK system is constructed, representing the two metro systems as interdependent complex networks and explicitly characterizing structural dependencies and flow-coupling mechanisms.
- A disaster-driven initial failure modeling approach is proposed based on scenario-specific extreme rainstorm parameters and station exposure indices, enabling the mapping of environmental shocks to network perturbations.
- A cascading failure dynamics model is developed by integrating load-capacity mechanisms with interdependent propagation rules, capturing the nonlinear diffusion processes within the cross-border coupled system.
- A multidimensional vulnerability assessment framework is established, combining structural vulnerability, functional vulnerability, and cascading vulnerability. In addition, a cross-border coupling amplification factor is introduced to quantify the amplifying effect of cross-border nodes during cascading processes.

This study develops a cross-border interdependency modeling framework to stress-test metro systems under extreme rainstorm scenarios. It provides a theoretical foundation for understanding systemic risks in cross-border critical infrastructure under extreme climate conditions and offers analytical and decision-making support for coordinated cross-border crisis management and resilience planning.

MODELING THE SZ-HK CROSS-BORDER METRO NETWORK

Complex Network Modeling of SZ Metro and HK MTR

As of June 2022, the Shenzhen Metro network (SZMN) comprised 12 lines, covering 240 stations, including 42

transfer stations (one four-line transfer station, four three-line transfer stations, and 37 two-line transfer stations). Meanwhile, the Hong Kong MTR network (MTRN) consisted of 10 lines and 97 stations, including 21 transfer stations (one four-line transfer station and 20 two-line transfer stations). As illustrated in Figure 1, all stations in the two metro networks are numbered sequentially by line. For transfer stations, their station *ID* is assigned according to the line with the smaller numerical label.

Based on complex network theory, this study adopts the *Space L* representation to construct the metro network models of Shenzhen and Hong Kong, denoted as G_A and G_B, respectively. Specifically, $G_A = (V_A, E_A)$ represents the SZMN, and $G_B = (V_B, E_B)$ represents the MTRN. The node set is defined as $V = \{v_i \mid i = 1,2, \dots, N\}$, and the edge set is defined as $E = \{e_{ij} \mid i, j = 1,2, \dots, N; i \neq j\}$, where $e_{ij} = (v_i, v_j)$ denotes a connection between two adjacent stations $i$and j. Figure 1 presents the spatial distribution of the two networks under the *Space L* modeling framework.

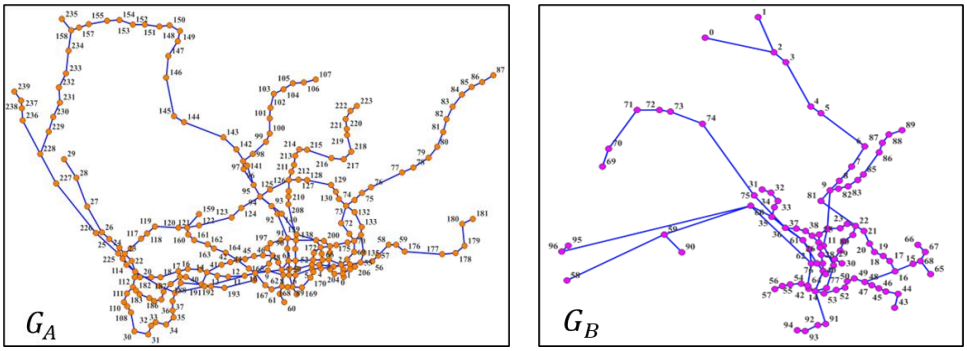

Figure 1. The encoded metro networks: SZMN (G_A) and MTRN (G_B).

Coupled Metro Network Modeling

Dual-Layer Network Representation

Although the SZMN and MTRN differ in operational management, regulatory frameworks, and infrastructure configurations, they are physically interconnected through a limited number of cross-border nodes (e.g., transfer stations and control points). To capture this hybrid structure, we abstract the SZMN and MTRN as a dual-layer interdependent network (as illustrated in Figure 2). Formally, the coupled system can be represented as $G = (G_A, G_B, D)$, where $D \subseteq V_A \times V_B$ denotes the set of cross-border coupling links. The overall node set is defined as $V = V_A \cup V_B$, with each node $v_i \in V_A \cup V_B$ corresponding to a metro station, and each edge representing a physical connection between adjacent stations.

At present, the top three cross-border checkpoints between Shenzhen and Hong Kong in terms of passenger flow are *Luohu Port*, *Shenzhen Bay Port*, and *Futian Port*. However, since there is no directly connected MTR station at *Shenzhen Bay Port*, cross-border travelers must transfer to shuttle buses, this study defines the cross-border coupling channels in the SZ-HK metro network as: (1) *Luohu*-SZ connected to *Lo Wu Station*-HK; and (2) *Futian Port*-SZ connected to *Lok Ma Chau Station*-HK (as indicated by the red double arrows in Figure 2). This dual-layer structure captures three key characteristics relevant to crisis management: administrative separation, physical interconnectivity, and functional interdependence. Unlike single-layer network models, the dual-layer structure explicitly captures cross-border interdependencies, enabling the analysis of interlayer cascading failures under extreme hazard conditions.

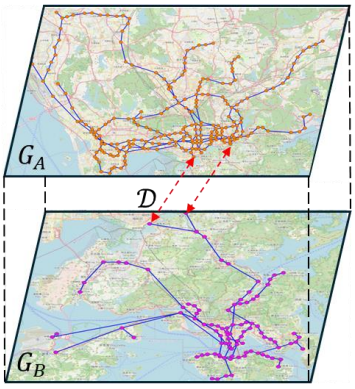

Figure 2. The SZ-HK coupled metro network.

Coupling Mechanisms

The interaction between the SZMN and the MTRN operates through two complementary coupling mechanisms: structural dependency and flow coupling. These mechanisms represent distinct pathways through which failures may propagate across the border.

Structural dependency captures the functional interconnections between adjacent cross-border stations. Let $i \in V_A$and $j \in V_B$ denote two stations linked via a cross-border interface. Their relationship is defined as $P(j \text{ fails} \mid i \text{ fails}) = q_{ij}$, where $q_{ij} \in [0,1]$ represents the dependency strength. When $q_{ij} = 1$, the two stations are fully interdependent, meaning that the closure of a station on one side necessarily results in functional failure of the corresponding station on the other side. Partial dependency ($0 < q_{ij} < 1$) reflects situations in which limited operations may still be maintained under constrained conditions. From a crisis management perspective, such structural dependency may arise from shared border inspection facilities, coordinated train dispatching constraints, or interoperability between control systems. This mechanism allows localized disruptions to directly trigger interlayer failures.

Flow coupling can capture indirect propagation driven by passenger flow redistribution. When a cross-border station becomes unavailable, displaced travel demand may shift to alternative cross-border nodes or parallel routes. Let ϕ denote the proportion of cross-border functional load relative to the total system load. If a cross-border node i fails, part of its load is redistributed to an alternative node k as $L_k \leftarrow L_k + \delta\phi L_i$, where L_i denotes the load proxy of node i and $\delta \in [0,1]$ represents the absorption ratio of alternative nodes. Flow coupling thus reflects a congestion amplification effect rather than direct structural failure. Even when structural dependency is relatively weak, load redistribution may still induce cascading failures through overload dynamics.

Topological Structure Measurement

In graph theory (Ermagun et al., 2023) and complex network analysis (Meng, 2024), node centrality measures constitute essential tools for examining topological characteristics and evaluating node importance within a network. In rail transit networks, node centrality reflects the extent to which a station is structurally connected to and interacts with other stations in the overall system. To date, numerous topological indicators have been developed to characterize the role of nodes from different analytical perspectives, and these measures have been extensively studied (Li et al., 2025). Commonly used centrality metrics include Degree Centrality, Eigenvector Centrality, Betweenness Centrality, Closeness Centrality, and PageRank. In this study, node centrality measures are employed to compare the structural importance of different stations within the SZMN and MTRN.

EXTREME RAINSTORM-DRIVEN CASCADING FAILURE FRAMEWORK

Extreme Rainstorm and Initial Failure Modeling

Hazard Scenario Construction

This study adopts a parameterized extreme rainstorm scenario modeling approach. By constructing a standardized rainfall process and multidimensional hazard intensity indicators, extreme rainstorms are represented as exogenous shock variables that can be directly input into the complex network cascading model. This approach

enables controlled comparisons of system responses under different hazard intensities, which is particularly valuable for emergency preparedness planning.

The extreme rainstorm hazard input vector is defined as:

$$H = \{I_{\max}, T, P, r, S, \eta\} \quad (1)$$

where $I_{\max}$ denotes peak rainfall intensity (mm/h), T denotes rainfall duration (h), P denotes cumulative precipitation (mm), r denotes relative timing of the peak intensity (0~1), S denotes spatial rainfall heterogeneity coefficient (dimensionless), and η denotes drainage system capacity attenuation coefficient (compound hazard parameter, 0~1). Among them, $I_{\max}$ and T characterize short-duration high-intensity impacts, reflecting the strength of the rainstorm; P captures system saturation and prolonged inundation effects; r describes the temporal structure of the rainfall process; S represents spatial heterogeneity; and η accounts for drainage capacity degradation under compound disaster scenarios. To ensure comparability across scenarios, continuous variables are normalized as follows:

$$\hat{I}_{\max} = \frac{I_{\max} - I_{\min}}{I_{\max} - I_{\min}}, \hat{T} = \frac{T - T_{\min}}{T_{\text{ref}} - T_{\min}}, \hat{P} = \frac{P - P_{\min}}{P_{\text{ref}} - P_{\min}} \quad (2)$$

To systematically characterize the impacts of different extreme rainfall patterns on the cross-border coupled system, a multidimensional composite scenario set $\mathcal{S}$ is constructed, where I_i, T_j, r_k correspond to hazard, S_m corresponds to exposure, and η_n corresponds to absorption capacity.

$$\mathcal{S} = \{I_i \times T_j \times r_k \times S_m \times \eta_n\} \quad (3)$$

Four intensity levels are defined: $\mathcal{S}_1$ (50-year return period), $\mathcal{S}_2$ (100-year return period), $\mathcal{S}_3$ (200-year return period), and $\mathcal{S}_4$ (500-year return period). These intensity levels are defined in relative terms and do not rely on specific city-based IDF (Intensity-Duration-Frequency) curve values, thereby preserving model generality. In addition, a standardized triangular rainfall hyetograph is adopted:

$$I(t) = \begin{cases} \dfrac{2I_{\max}}{rT}\, t, & 0 \le t < rT \\ \dfrac{2I_{\max}}{(1-r)T}\,(T-t), & rT \le t \le T \end{cases} \quad (4)$$

The parameter $r \in (0,1)$ controls the timing of peak intensity. Specifically, $r = 0.3$ (early peak), $r = 0.5$ (mid-peak), and $r = 0.7$ (late peak) are selected to reflect how different rainfall temporal structures influence drainage system response and, consequently, system vulnerability.

Station Exposure and Vulnerability Function

This study adopts a three-stage hazard-exposure-vulnerability mapping framework (Guo et al., 2025; Wu et al., 2024) to translate rainstorm scenarios into the initial failure probabilities of metro stations.

Relevant station-level indicators are considered, including: underground & elevated station status $\text{Und}_i \in \{0,1\}$, transfer station status $\text{Hub}_i \in \{0,1\}$, entrance number $\text{Ent}_i \in \{1,2,3\}$, topographic classification (low-lying/normal/elevated) $\text{Low}_i \in \{1,2,3\}$, and proximity to flood-prone areas $\text{Wat}_i \in \{1,2,3\}$. After normalization, these indicators are linearly aggregated to construct the exposure-sensitivity index for station i:

$$E_i = \sum_{k=1}^{K} \beta_k \tilde{x}_{ik} \quad (5)$$

where $\tilde{x}_{ik}$ denotes the normalized station attribute indicators, and β_k represents the corresponding weights, satisfying $\sum \beta_k = 1$. The weights are determined using a weighted TOPSIS method (Meng, 2024), and their robustness is examined through sensitivity analysis.

The scenario intensity is then coupled with the station exposure index $E_i$to define the composite hazard level of station i under scenario s, denoted as $X_i(s)$. Let ω represent the weights of different hazard factors, and $X_i(s)$ captures the disaster intensity experienced by station i under a specific scenario. The hazard level is formulated as:

$$X_i(s) = E_i \cdot \left(\omega_I \hat{I}_{\max} + \omega_P \hat{P} + \omega_T \hat{T}\right) \cdot (1 + \omega_S S) \cdot (1 + \omega_\eta \eta) \quad (6)$$

A Logistic vulnerability function is employed to describe the relationship between hazard intensity and failure probability:

$$p_i(s) = \frac{1}{1 + \exp\left[-a(X_i(s) - b)\right]} \quad (7)$$

where a denotes the slope parameter, reflecting the uncertainty of station failure, and b represents the median failure threshold, indicating the overall flood protection capacity of the system. This probabilistic formulation captures the inherent uncertainty in infrastructure response and enables scenario-based Monte Carlo simulations. Under intense rainfall conditions, stations with higher exposure levels exhibit a greater likelihood of failure.

For each scenario, Monte Carlo sampling is applied to generate the initial failure state of each station $F_i^{(0)} \sim \text{Bernoulli}(p_i(s))$, yielding the initial failure set $F_0(s) = \{i \mid F_i^{(0)} = 1\}$ under scenario s. This set serves as the exogenous trigger node set for subsequent cascading failure simulations.

Cascading Failure Dynamics in Cross-Border Coupled Systems

Load-Capacity Mechanism

In metro systems, the functionality of a station depends on its ability to handle passenger flows and coordinate operations. When a station becomes inoperative, passenger demand is redistributed to adjacent stations, potentially increasing operational pressure. In this study, betweenness centrality (BC) is adopted as a proxy variable for node load:

$$L_i^0 = \text{BC}_i \quad (8)$$

where $\text{BC}_i = \sum_{s \neq i \neq t} \frac{\sigma_{st}(i)}{\sigma_{st}}$, σ_{st} denotes the total number of shortest paths between nodes $s$and t, and $\sigma_{st}(i)$ represents the number of those paths that pass through node i. To avoid scale effects, the load is normalized as $\tilde{L}_i^0 = \frac{L_i^0}{\max_j L_j^0}$. This approach captures the structural importance and potential load level of nodes in the absence of observed origin-destination passenger flow data.

A classical load-capacity model (Wang et al., 2025) is employed:

$$C_i = (1 + \alpha)\tilde{L}_i^0 \quad (9)$$

where $\alpha \in [0.1, 0.5]$ is a redundancy coefficient representing the overall buffering capacity of the system. Considering that underground stations may experience capacity degradation under extreme rainfall conditions, the effective capacity is defined as:

$$C_i^{\text{eff}} = (1 - \rho_i)C_i \quad (10)$$

where ρ_i denotes the rainstorm-induced capacity reduction coefficient, determined by station type and equipment exposure conditions.

Cascade Failure Propagation Mechanism

The cascading failure process of the metro network under extreme rainstorm scenarios is divided into two stages: exogenous triggering and endogenous diffusion. For each scenario s, the cascading process is modeled as Table 1. This iterative process captures the nonlinear cascading dynamics arising from load redistribution and capacity constraints under extreme rainfall disturbances.

Table 1. The cascading failure propagation process

Start
Step 0: Initial Disaster-Induced Failures • For each station i, determine whether a disaster-triggered failure occurs by sampling according to $p_i(s)$. • Remove the failed nodes in the initial failure set $F_0(s)$ from the network.
Step 1: Load Redistribution • After node removals, the remaining stations must absorb the redistributed flow pressure. • Recalculate the proxy load in the residual network: $\tilde{L}_i^{(t)} = \text{BC}_i^{(t)}$, where t denotes the cascade iteration step, and betweenness centrality is recomputed at each round based on the current remaining network structure.

Step 2: Overload Criterion

- If a node satisfies $\tilde{L}_i^{(t)} > C_i^{\text{eff}}$, it is deemed to experience overload failure at iteration t.
- The newly failed node set is defined as $F_t = \{i \mid \tilde{L}_i^{(t)} > C_i^{\text{eff}}\}$

Step 3: Iteration Until Convergence

- Repeat Steps 1~2 until no additional failures occur (i.e., $F_t = \emptyset$) or the network collapses.

End

Modeling of Cross-Border Coupling Effects

To model the cross-border coupling effects in the SZ-HK dual-layer metro network, this study introduces two key parameters: structural interdependence strength q and flow coupling proportion ϕ. It should be emphasized that q and ϕ are control parameters within the cascading propagation dynamics model, rather than endogenous system state variables.

For each cross-border coupled node pair ($i \in V_A, j \in V_B$), the dependency strength is denoted as q_{ij}. If node $i$fails, the effective capacity of node $j$is reduced according to $C_j^{\text{eff}} \leftarrow (1 - q_{ij})C_j^{\text{eff}}$, when $q_{ij} = 1$, the two nodes are fully interdependent, implying complete functional reliance across the border.

In addition, a cross-border flow proportion parameter ϕ is defined. When a cross-border node fails, a portion of its load is redistributed to alternative nodes according to $\tilde{L}_k^{(t)} \leftarrow \tilde{L}_k^{(t)} + \delta\phi\tilde{L}_i^{(t-1)}$, where δ denotes the flow absorption ratio of substitute nodes. This mechanism captures the risk of secondary overload arising from cross-border alternative routes.

The coexistence of load redistribution and structural interdependence gives rise to nonlinear amplification effects. Depending on system redundancy, dependency strength, and cross-border flow proportion, the coupled system may exhibit localized containment, progressive degradation, or systemic collapse. Such regime-shift behavior is particularly significant for crisis management, as small variations in coupling strength can lead to fundamentally different systemic outcomes.

MULTIDIMENSIONAL VULNERABILITY ASSESSMENT

Vulnerability Assessment Framework

Although cascading mechanisms describe how disruptions propagate, decision-makers require interpretable metrics to quantify the extent of system damage (Lu et al., 2022). We construct a multidimensional vulnerability assessment framework, encompassing topological structural vulnerability, network functional vulnerability, and cascading propagation vulnerability, to evaluate the impacts of extreme rainstorm-induced cascading failures in the cross-border metro system. This framework further enables identification of the vulnerability amplifier effect associated with cross-border nodes.

Let scenario $s \in \mathcal{S}$. After the cascading process converges, the post-disruption network is denoted as $G^{\text{post}}(s)$, and the initial intact network as G^{pre}. The three-dimensional vulnerability vector is defined as

$$V(s) = (V_S(s), V_F(s), V_C(s)) \tag{11}$$

Where structural vulnerability V_S measures the degradation of connectivity and topological efficiency in the cross-border network; functional vulnerability V_F quantifies the decline in functional performance and service efficiency; cascading vulnerability V_C evaluates the scale, depth, and threshold sensitivity of failure diffusion triggered by extreme rainstorms. The quantitative indicators and corresponding computational methods for these three dimensions are summarized in Table 2.

Table 2. The scoring standard of emergency capability evaluation

Dimension	Index	Calculation	Explanation
Structural vulnerability	The loss rate of largest connected component V_{S1}	$V_{S1}(s) = 1 - \frac{\mid LCC^{post}(s) \mid}{\mid LCC^{pre} \mid}$	It measures the extent of network fragmentation.
	The loss rate of network efficiency V_{S2}	$E(G) = \frac{1}{N(N-1)} \sum_{i \neq j} \frac{1}{d_{ij}}$ $V_{S2}(s) = 1 - \frac{E(G^{post}(s))}{E(G^{pre})}$	It captures the decline in overall network accessibility.
	The increase of average path length V_{S3}	$V_{S1}(s) = 1 - \frac{\mid LCC^{post}(s) \mid}{\mid LCC^{pre} \mid}$	It measures the degree of increase in the rerouting cost of the network.
Functional vulnerability	The loss rate of OD connectivity pair V_{F1}	$V_{F1}(s) = 1 - \frac{\left\mid \{(i,j): i \neq j, d_{ij}^{post}(s) < \infty \mid \right.}{\left\mid \{(i,j): i \neq j, d_{ij}^{pre} < \infty \mid \right.}$	It reflects the availability of cross-border services.
	The loss rate of cross-border accessibility V_{F2}	$V_{F2}(s) = 1 - \frac{\left\mid \{(i,j): i \in A, j \in B, d_{ij}^{post}(s) < \infty\} \right\mid}{\mid A \mid \cdot \mid B \mid}$	It indicates the degradation of cross-border mobility.
	The loss of alternative path capability V_{F3}	$V_{F3}(s) = 1 - \frac{\kappa^{post}(s)}{\kappa^{pre}}$	It represents the reduction in network redundancy.
Cascading vulnerability	Final failure scale V_{C1}	$V_{C1}(s) = \frac{\mid V_{fail}(s) \mid}{N}$	It measures the system's ability to resist chain reactions.
	Cascade propagation depth V_{C2}	$V_{C2}(s) = \frac{T_c(s)}{T_{\max}}$	It reflects the system's diffusion capability.
	Endogenous diffusion gain V_{C3}	$V_{C3}(s) = \frac{\mid \mathcal{F}_\infty(s) \mid - \mid \mathcal{F}_0(s) \mid}{N}$	It measures the additional failures caused by cascading.

To ensure comparability across indicators with different units and magnitudes, min-max normalization is applied:

$$\tilde{V}_k(s) = \frac{V_k(s) - \min_s V_k(s)}{\max_s V_k(s) - \min_s V_k(s)} \quad (12)$$

The overall composite vulnerability index is then defined using a vector norm form to avoid introducing subjective weighting uncertainty. This formulation enables a quantitative assessment of vulnerability in the SZ-HK cross-border coupled metro system.

$$V_{\text{all}}(s) = \| \mathbf{V}(s) \|_2 = \sqrt{\tilde{V}_S^2 + \tilde{V}_F^2 + \tilde{V}_C^2} \quad (13)$$

Coupling Amplifier Effect

To clarify the role of cross-border coupling, we compare system vulnerability under coupled and decoupled configurations. The amplification factor induced by coupling is defined as:

$$AF = \frac{V_{\text{all}}^{\text{coupled}} - V_{\text{all}}^{\text{decoupled}}}{V_{\text{all}}^{\text{decoupled}}} \tag{14}$$

A positive AF indicates that cross-border coupling amplifies overall system vulnerability beyond that observed in isolated metro systems. This metric quantitatively captures the vulnerability amplification effect of cross-border nodes and provides a basis for identifying critical cross-jurisdictional coordination requirements in crisis management.

PRELIMINARY INSIGHTS, IMPLICATIONS AND FUTURE WORK

Conceptual Validation and Preliminary Results

Simplified Network Design

To validate the internal consistency of the proposed cascading failure model and to illustrate the cross-border amplification mechanism in a transparent manner, we construct a synthetic 14-node dual-layer metro network. As shown in Figure 3, the network consists of two layers, with seven stations in each layer (SZ layer: A1~A7 and HK layer B1~B7). Within each layer, stations are arranged into two intersecting lines connected by a central hub (A3 and B3), forming a small but non-trivial multi-line structure capable of supporting alternative routing and load redistribution.

Two cross-border physical connectors are introduced: a primary cross-border hub (A3~B3) and a secondary connector (A7~B7). These connectors represent major and auxiliary cross-border interchange channels. Structural interdependency is imposed on both cross-border station pairs, such that failure of one station may probabilistically trigger failure of its counterpart with strength q. In addition, cross-border flow coupling is modeled through a redirection mechanism: when one cross-border connector fails, a proportion of its load is transferred to the alternative connector, potentially inducing overload.

The simplified network is intentionally minimal to ensure interpretability while preserving essential mechanisms of intra-layer routing, cross-layer physical connectivity, probabilistic interdependency, and overload-driven cascading. This design enables controlled exploration of how extreme rainstorm-induced disruption at a critical cross-border hub propagates across layers and amplifies systemic vulnerability.

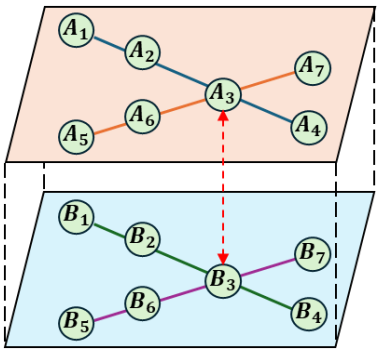

Figure 3. The dual-layer simplified network structure.

Experimental Setup

The conceptual validation experiment is designed to examine whether the proposed model can reproduce cross-border amplification effects and redundancy threshold behavior under controlled conditions.

An extreme rainfall scenario is represented by the initial failure of the primary cross-border hub (A3), reflecting a localized but strategically important disruption. Cascading dynamics then unfold according to the proposed mechanism: dependency-triggered failures, cross-border load redistribution, dynamic betweenness-based load recalculation, and overload-induced node removal. To quantify amplification, we compare a coupled configuration (including cross-border physical edges, interdependency, and flow coupling) with a decoupled

baseline in which cross-border physical connectors are removed and both dependency and flow coupling are disabled. The amplification factor AF is computed as the relative increase in composite vulnerability between the two configurations.

The parameter settings are specified as follows. The dependency strength q is defined over the interval [0,1] and is systematically varied to represent different levels of inter-system coupling between cross-border stations, enabling analysis of its influence on the amplification factor (i.e., the $AF \sim q$ relationship). The flow coupling parameters ϕ and δ are assigned relatively high values (e.g., $\phi = 0.9$, $\delta = 1.0$) to emulate stress conditions in which disrupted passenger flows are predominantly redirected to alternative connectors with minimal dissipation. The redundancy parameter α serves as a control variable governing node capacity and is varied over a wide range to identify threshold behavior in cascading failures (i.e., the $V_{C1} \sim \alpha$ relationship). For each parameter configuration, Monte Carlo simulations with multiple random seeds are conducted to capture stochastic interdependency effects, and the averaged multidimensional vulnerability metrics (V_S, V_F, and V_C) are reported.

Key Observations

The conceptual validation results for the 14-node dual-layer simplified network under dynamic load redistribution are presented in Figures 4~6.

As shown in Figure 4, the comparison of V_S, V_F, and V_C indicates that the coupled cross-border configuration produces substantially greater multidimensional degradation than the decoupled baseline. Specifically, the coupled case exhibits pronounced structural vulnerability ($V_S = 0.834$), functional vulnerability ($V_F = 0.798$), and cascading vulnerability ($V_C = 0.213$), whereas the decoupled configuration remains markedly less affected ($V_S = 0.161$, $V_F = 0.558$, $V_C = 0.035$). This gap indicates that localized rainfall-induced disruption at the primary cross-border hub can escalate into system-wide fragmentation and service loss when cross-border physical connectivity, interdependency, and load-transfer mechanisms are present.

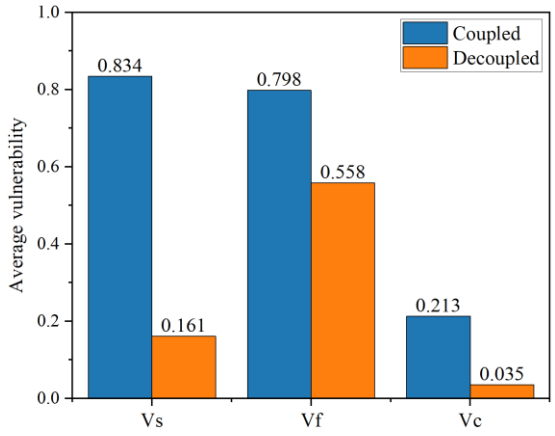

Figure 4. The simulation results of V_S, V_F, and V_C.

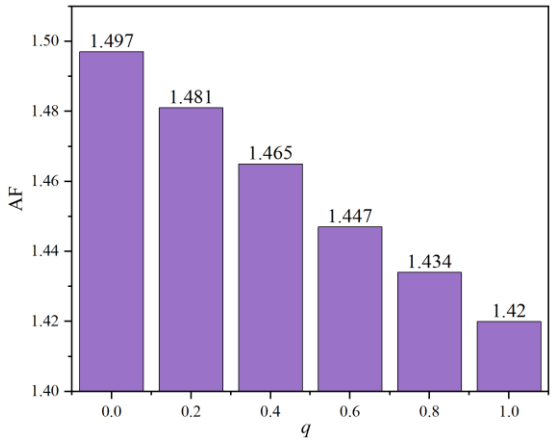

Figure 5. The simulation results of AF and q.

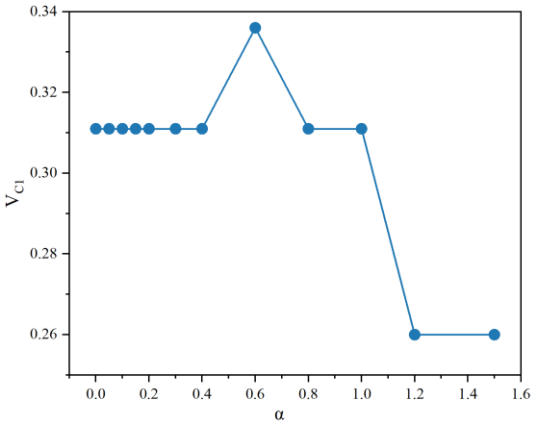

Figure 6. The simulation results of V_{C1} and α.

Figure 5 illustrates the $AF \sim q$ relationship, further confirming a robust cross-border amplification effect. The amplification factor AF remains strongly positive across the entire range of dependency strength ($AF \approx 1.42 \sim 1.50$), suggesting that neglecting cross-border coupling would lead to a substantial underestimation of systemic vulnerability. The slight decrease of AF with increasing q reflects a diminishing marginal effect of interdependency strength under this simulation environment, where the dominant amplification is driven by cross-border connectivity and overload-mediated redistribution rather than by interdependency alone.

The $V_{C1} \sim \alpha$ curve shown in Figure 6 reveals threshold-like redundancy behavior. The final failure ratio V_{C1} remains on a high plateau under low-to-moderate redundancy ($\alpha \leq 1.0$; $V_{C1} \approx 0.31$), but drops to a lower plateau once redundancy exceeds a critical level ($\alpha \geq 1.2$; $V_{C1} \approx 0.26$). This pattern is consistent with a regime shift from overload-prone cascading dynamics to a mitigated propagation state.

Overall, these preliminary results demonstrate that cross-border connectors can act as systemic vulnerability amplifiers through the combined pathways of interdependency-triggered failures and overload-driven load redistribution, and that sufficient redundancy at key cross-border nodes is crucial for containing cascading risks under extreme rainstorms.

Implications for Crisis Management

The conceptual validation results provide several implications for cross-border crisis management under extreme rainstorm conditions, while highlighting the contributions of this study relative to existing interdependency research.

- First, the consistently positive amplification factor ($AF > 0$) indicates that cross-border coupling significantly increases systemic vulnerability compared with isolated metro systems. While prior studies mainly classify interdependencies, our results quantify how such coupling amplifies cascading impacts, suggesting that independent risk assessments may underestimate system-wide disruptions and underscoring the need for joint cross-border contingency planning.
- Second, the observed divergence between structural (V_S) and functional (V_F) degradation shows that connectivity alone is insufficient to assess system performance under crisis conditions. This extends existing studies by emphasizing functional indicators, such as cross-border accessibility and alternative routing capacity, as critical metrics for operational decision-making.
- Third, the threshold behavior in the $V_{C1} \sim \alpha$ curve reveals a transition between cascade-prone and cascade-resistant regimes. This provides actionable insights beyond traditional interdependency analysis by identifying minimum redundancy levels required to contain cascading failures, supporting targeted resilience investments at key cross-border nodes.
- Finally, the results demonstrate that cross-border connectors act as systemic vulnerability amplifiers through interdependency and load redistribution. From a crisis management perspective, these nodes should be treated as critical coordination points rather than purely physical infrastructure. The proposed framework can therefore support scenario-based risk assessment and cross-border coordination within crisis management information systems.

Ongoing and Future Work

While the simplified network validation confirms the internal consistency and theoretical plausibility of the proposed modeling framework, several extensions are necessary to enhance empirical realism and decision relevance. The ongoing and future work is summarized as follows:

- Future work will incorporate detailed network data from the Shenzhen and Hong Kong metro systems to construct a higher-resolution dual-layer network representation. This will enable the study of spatial heterogeneity, multi-line redundancy patterns, and multiple cross-border interconnection structures beyond the scope of the simplified model.
- The current rainfall-induced failure modeling relies on abstract initial node removal. Ongoing research aims to integrate spatially explicit rainfall scenarios and station-level exposure parameters, enabling more realistic mapping from hazard intensity to initial disruption sets. This integration will support scenario-based stress testing under varying rainfall return periods.
- The present model uses betweenness centrality as a proxy for load in the absence of real passenger flow data. Future work will explore the incorporation of empirical or synthetic demand matrices to refine overload dynamics and improve functional performance evaluation.
- Further sensitivity analysis is required to systematically explore the interaction between dependency strength, flow coupling intensity, and redundancy levels. Identifying phase-transition boundaries in larger-scale networks may provide more generalizable insights into critical resilience thresholds.
- Finally, subsequent research will examine governance-level coupling, including cross-border information sharing, coordinated dispatching strategies, and adaptive control policies. Embedding such organizational dimensions into the interdependent network framework may help bridge the gap between infrastructural vulnerability modeling and operational crisis management practice.

Together, these extensions aim to transform the present conceptual validation into a comprehensive decision-support framework for assessing and mitigating cascading risks in cross-border metro systems under extreme climate events.

CONCLUSIONS

This study develops a network-based cascading vulnerability assessment framework for cross-border metro systems under extreme rainstorm, focusing on the Shenzhen-Hong Kong context. Building on interdependency theory, the model integrates structural dependency and dynamic load redistribution to capture both dependency-triggered and overload-driven cascading mechanisms. Conceptual validation on a dual-layer simplified network shows that cross-border coupling amplifies system-wide degradation and exhibits threshold-like behavior with respect to redundancy. These results indicate that cross-border connectors act as vulnerability amplifiers and that sufficient redundancy at key hubs is critical for cascading failures. Compared with existing interdependency studies, this study links interdependency structures with dynamic cascading processes and provides quantitative indicators (e.g., amplification effects and resilience thresholds) relevant for crisis management. The framework can support scenario-based risk assessment and cross-border coordination within crisis management information systems. As a work-in-progress study, this research establishes a theoretical foundation. Future work will incorporate empirical metro data and rainfall scenarios to enable calibrated analysis and actionable decision-making support for coordinated cross-border crisis management under extreme climate events.

ACKNOWLEDGMENTS

This work is supported by the National Natural Science Foundation of China (Grand No. 72304126). We thank the editors and reviewers for the valuable comments.

REFERENCES

Ansari, A., Thadagani, K. S., Seshagiri Rao, K., Shekhar, S., & Alluqmani, A. E. (2024). Assessing seismic vulnerability in metro systems through numerical modeling: Enhancing the sustainability and resilience of urban underground utilities (3U). *Innovative Infrastructure Solutions*, *9*(10), 366. https://doi.org/10.1007/s41062-024-01685-1

Borghetti, F., & Marchionni, G. (2023). Cross-border critical transportation infrastructure: A multi-level index for resilience assessment. *Transportation Research Procedia*, *69*, 77–84. https://doi.org/10.1016/j.trpro.2023.02.147

Chen, Z., Zheng, C., Xu, M., Du, M., Ma, J., & Zheng, S. (2024). Reliability of urban underground-aboveground logistics networks under rainfall-flood and cascading failure scenarios. *Transportation Research Part D: Transport and Environment*, *136*, 104480. https://doi.org/10.1016/j.trd.2024.104480

Ermagun, A., Tajik, N., Janatabadi, F., & Mahmassani, H. (2023). Uncertainty in vulnerability of metro transit networks: A global perspective. *Journal of Transport Geography*, *113*, 103710. https://doi.org/10.1016/j.jtrangeo.2023.103710

Gao, W., Lu, Y., Wang, N., Cheng, G., Qiu, Z., & Hu, X. (2024). Measurement and prediction of subway resilience under rainfall events: An environment perspective. *Transportation Research Part D: Transport and Environment*, *136*, 104479. https://doi.org/10.1016/j.trd.2024.104479

Guo, C., Tang, J., Hong, J., Lu, Q., Wu, H., & Wei, R. (2025). Resilience assessment of urban bus-metro system to floods under future climate change. *Transportation Research Part D: Transport and Environment*, *148*, 104925. https://doi.org/10.1016/j.trd.2025.104925

Hong, W.-T., Clifton, G., & Nelson, J. D. (2022). Rail transport system vulnerability analysis and policy implementation: Past progress and future directions. *Transport Policy*, *128*, 299–308. https://doi.org/10.1016/j.tranpol.2022.02.004

Huang, Z., & Loo, B. P. Y. (2023). Urban traffic congestion in twelve large metropolitan cities: A thematic analysis of local news contents, 2009–2018. *International Journal of Sustainable Transportation*, *17*(6), 592–614. https://doi.org/10.1080/15568318.2022.2076633

Jiao, L., Zhu, Y., Huo, X., Wu, Y., & Zhang, Y. (2023). Resilience assessment of metro stations against rainstorm disaster based on cloud model: A case study in Chongqing, China. *Natural Hazards*, *116*(2), 2311–2337. https://doi.org/10.1007/s11069-022-05765-2

Jing, D., Li, W., Wen, J., Hou, W., Wu, H., Liu, J., Zhang, M., Zhang, W., Tian, T., Ding, Z., & Guo, H. (2025). Critical node failure, impact and recovery strategy for metro network under extreme flooding in Shanghai. *International Journal of Disaster Risk Reduction*, *121*, 105414. https://doi.org/10.1016/j.ijdrr.2025.105414

Li, J., Luo, Y., Ou, J., Zhou, S., Lu, C., & Zhou, Y. (2025). Assessing the robustness of urban metro networks under flooding risk. *Transportation*, 1–35. https://doi.org/10.1007/s11116-025-10673-y

Liang, C., & Guan, M. (2025). Increasing flood hazards threaten metro system resilience under climate and demographic changes. *Sustainable Cities and Society*, *133*, 106890. https://doi.org/10.1016/j.scs.2025.106890

Liang, C., Guan, M., Guo, K., Yu, D., & Yin, J. (2026). Dynamic flood risk modeling in urban metro systems considering station configuration. *Reliability Engineering & System Safety*, *266*, 111760. https://doi.org/10.1016/j.ress.2025.111760

Lu, Q.-C., Zhang, L., Xu, P.-C., Cui, X., & Li, J. (2022). Modeling network vulnerability of urban rail transit under cascading failures: A Coupled Map Lattices approach. *Reliability Engineering & System Safety*, *221*, 108320. https://doi.org/10.1016/j.ress.2022.108320

Ma, Z., Liu, J., Chien, S. I.-J., Hu, X., & Shao, Y. (2023). Identifying Critical Stations Affecting Vulnerability of a Metro Network Considering Passenger Flow and Cascading Failure: Case of Xi'an Metro in China. *ASCE-ASME Journal of Risk and Uncertainty in Engineering Systems, Part A: Civil Engineering*, *9*(2), 04023014. https://doi.org/10.1061/AJRUA6.RUENG-1013

Meng, Y. (2024). Vulnerability Comparisons of Various Complex Urban Metro Networks Under Multiple Failure Scenarios. *Sustainability*, *16*(21), 9603. https://doi.org/10.3390/su16219603

Qi, Q., Meng, Y., Zhao, X., & Liu, J. (2022). Resilience Assessment of an Urban Metro Complex Network: A Case Study of the Zhengzhou Metro. *Sustainability*, *14*(18), 11555. https://doi.org/10.3390/su141811555

Rinaldi, S. M., Peerenboom, J. P., & Kelly, T. K. (2001). Identifying, understanding, and analyzing critical infrastructure interdependencies. *IEEE Control Systems*, *21*(6), 11–25. https://doi.org/10.1109/37.969131

Tian, R., Zhang, Y., Peng, L., Wang, Y., Wang, W., & Gu, Y. (2024). Measurement of flood resilience of metro station based on combination weighting-cloud model. *International Journal of Disaster Risk Reduction*, *114*, 104950. https://doi.org/10.1016/j.ijdrr.2024.104950

Wang, Y., Ye, Z., Jia, X., Liu, H., Zhou, G., & Wang, L. (2025). Flood disaster chain deduction based on cascading failures in urban critical infrastructure. *Reliability Engineering & System Safety*, *261*, 111160. https://doi.org/10.1016/j.ress.2025.111160

Wu, J., Ma, L., Guo, F., Chen, K., & Fang, W. (2024). An MCDM-GIS framework for assessing flooding resilience of urban metro systems. *International Journal of Disaster Risk Reduction*, *113*, 104824. https://doi.org/10.1016/j.ijdrr.2024.104824

Yang, X., Zhang, X., Li, S., Tian, Y., Tan, C., Ding, S., Kalonji, G., & Xu, L. (2025). Increasing urban flooding facing metro system: Evidence from Internet media records in China from 2001 to 2021. *International Journal of Disaster Risk Reduction*, *124*, 105551. https://doi.org/10.1016/j.ijdrr.2025.105551

Zhang, D.-M., Bai, H., Zheng, C.-Z., Huang, H.-W., Ayyub, B. M., & Cao, W.-J. (2025). Extreme rainfall induced risk mapping for metro transit systems: Shanghai metro network as a case. *Reliability Engineering & System Safety*, *262*, 111234. https://doi.org/10.1016/j.ress.2025.111234

Zhang, J., Wang, S., & Wang, X. (2018). Comparison analysis on vulnerability of metro networks based on complex network. *Physica A: Statistical Mechanics and Its Applications*, *496*, 72–78. https://doi.org/10.1016/j.physa.2017.12.094

Zhang, Y., Ayyub, B. M., Saadat, Y., Zhang, D., & Huang, H. (2020). A double-weighted vulnerability assessment model for metrorail transit networks and its application in Shanghai metro. *International Journal of Critical Infrastructure Protection*, *29*, 100358. https://doi.org/10.1016/j.ijcip.2020.100358